Geotechnical Aspects of Underground Construction in Soft Ground – Ng, Huang & Liu (eds)
© 2009 Taylor & Francis Group, London, ISBN 978-0-415-48475-6

Floor heave behavior and control of roadway intersection in deep mine

B.H. Guo & T.K. Lu
School of Energy Science & Engineering, Henan Polytechnic University, Jiaozuo, Henan, P.R.China

ABSTRACT: For investigating floor heave behavior and controlling technique of roadway intersection in deep mine, creep deformation characteristics of floor around roadway intersection was studied by Flac^{3D} and the effects of shear plastic critical value, reinforcement measurement on creep deformation of floor around roadway intersection were discussed. As a result, the creep deformation curve can be divided into two stages including initial creep deformation stage and softening deformation stage, which can explain the case that deformation of roadway intersection is little before a certain time, but then increases at a high speed; only when total shear plastic value exceeds the critical value can second creep stage take place; reinforcement measurement with bolting in roof and ribs has little effect on floor heave, yet exerting pressure against floor can reduce floor heave obviously.

1 INTRODUCTION

Rocks mass of roadway in deep mine show soft behavior because they are located in high stress environment. Due to its larger cross section and complex geometries deformation of floor around roadway intersection is usually greater than roadway doesn't intersect. Floor heave has a great influence on ventilation, transportation, and so on, thus a lot of literatures already exist about this issue, but there are only a few in which was based on alternating effects between softening and creeping (Yang et al. 2006).

Strata of North ventilation roadway at −990 m level in Tangkou colliery is silty mud rock in mainly green and cinereous, mingled with a little fine sand rock at some locality. Protodrakonov scale of hardness f is 2.2, pressive strength is 19 MPa, and tensile strength ranges from 1.67 MPa to 4.45 MPa. The burial depth of roadway is nearly from 1029 m to 1035 m, maximum main stress is about 31.6 MPa, and the vertical stress is between 25 MPa and 26 MPa (Liu et al. 2005), which is larger than its pressive strength, thus softening deformation and creeping deformation will occur simultaneously (Wang et al. 1994). A case has been observed that the deformation of roadway intersection was less before about the 45th day after it was formed, but then accelerated and convergence between roof and floor reached 565 mm at the 90th day, among which floor heave accounted for more than 70 percent. Therefore, behavior and controlling technique of roadway intersection in deep mine was investigated according to conditions of a roadway intersection at −990 m level in Tangkou colliery, with effects of softening/creeping of rocks mass interaction being considered by means of numerical simulation method.

2 NUMERICAL SIMULATIONS PROCEDURE

2.1 *Failure criteria*

Pwipp model (a visco-plastic model combining WIPP model (the rock creep visco-elastic model) and the Drucker-Prager model) is used in this study. Total strain includes deviate strain and average strain. Deviated strain contains three components of elastic strain, plastic strain and viscosity strain, while average strain contains two components mentioned above except for viscosity strain (Liu et al. 2005).

Strength of rocks mass decreases gradually along with development of deformation after rocks mass begin to failure (Wang et al. 2006), and the bearing capacity of rocks mass in plastic regions is lower than in elastic regions. Cohesion and friction angle lower at different degrees (Xiao et al. 2005, Zhang et al. 2005) along with development of plastic deformation, residual cohesion will lost totally and bearing capacity is provided by only friction force (You 2005). Therefore, strain-softening model can be used to study deformation of roadway intersection undoubtedly (Yang et al. 2002).

Change of strain especially plastic strain externalizes the loading path and history, and reflects softening process of material from initial condition to final failure (Zheng 2007). Referring to relationship between softening process and plastic deformation (see Fig.1) from You (2000), Diagrammatic sketch of full shear plastic strain-softening curve (see Fig. 2a) was got. Figure 2a shows that the softening coefficients of strength k (the ratio of stress corresponding to plastic strain to strength peak value) increases with shear plastic strain when shear plastic strain is below ε_{p1},

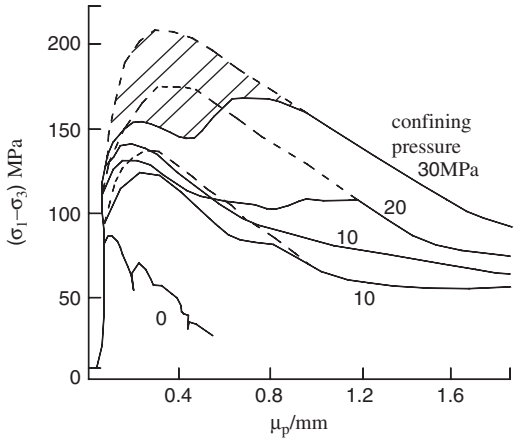

Figure 1. Relationship between softening process and plastic deformation (after You, 2000).

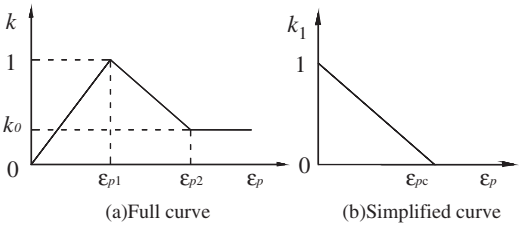

Figure 2. Diagrammatic sketch of softening coefficient-shear plastic strain curve.

decrease when the shear plastic strain is between ε_{p1} and ε_{p2}, and keep unchanged as a constant value k_0 when shear plastic strain is above ε_{p2}. Because ε_{p1} and k_0 are usually very little, they are both assumed as 0 here, thus the simplified shear plastic strain-softening curve (see Fig. 2b) was obtained. Besides, when total strain of rocks mass exceeds the strain value at peak strength, deformation modulus lessen gradually with strain, but residual deformation modulus is never reach 0 (see Fig. 3).Other researchers (Zeng et al. 2005, Liang et al. 2005, Cheng et al. 2005, Chen et al. 2005, Li et al. 2006, Qiang et al. 2006, Wang et al. 2007) also reported the similar opinion.

If we define k_1 as strength softening coefficient and k_2 as deformation softening coefficient, they can be defined by following formulas:

$$\begin{cases} k_1 = 1 - \dfrac{\varepsilon_p}{\varepsilon_{pc}} & 0 < \varepsilon_p \le \varepsilon_{pc} \\ k_1 = 0 & \varepsilon_p > \varepsilon_{pc} \end{cases} \quad (1)$$

$$\begin{cases} k_2 = 0.8 & 0 < \varepsilon_p \le \varepsilon_{pc} \\ k_2 = 0.5 & \varepsilon_p > \varepsilon_{pc} \end{cases} \quad (2)$$

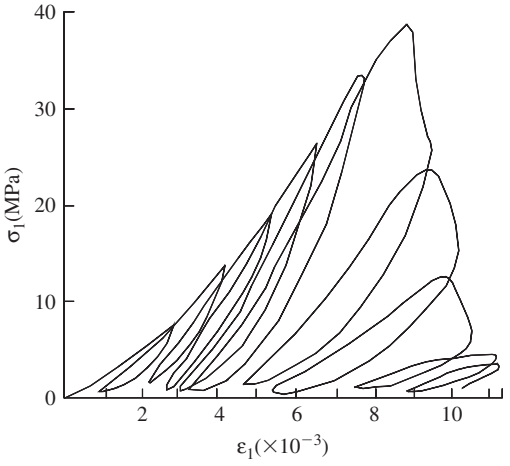

Figure 3. Stress-strain curves under cycle loading (after Zhu, 1985).

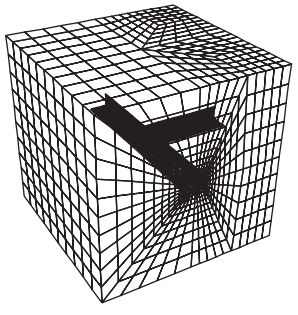

Figure 4. Simulated model.

where ε_p = shear plastic value; and ε_{pc} = shear plastic critical value, 2e-3 here.

2.2 *Model development*

Assumption of rocks mass being homogeneous and in hydrostatic-pressure state was made in this work. Simulated model containing a T shaped roadway intersection and bolt supporting sketch were plotted in Figure 4 and Figure 5 respectively. The sizes of calculated model were 40 m length, 40 m width and 40 m height. The bottom of the model was fixed in all directions, four sides were fixed in horizontal direction, and overburden weight was exerted on the top of the model. The section of roadway was rectangle with width of 4 m and height of 3 m. The length and diameter of 2 anchors bolted in the roof were 6300 mm and 17.8 mm respectively, the interval along the axial and circumferential direction of the roadway were 3000 mm and 2400 mm respectively; for cables, the corresponding values were 2300 mm, 18 mm, 1000 mm and 1200 mm

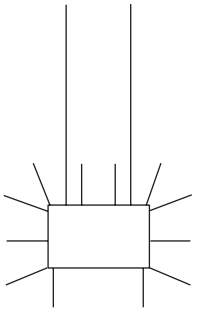

Figure 5. Bolt supporting sketch.

Table 1. Mechanical parameters of rocks mass.

Parameters	Bulk modulus K	Shear modulus G	Density D	Shear strength τ_f	Tensile strength σ_t
Units	GPa	GPa	kg/m^3	MPa	MPa
Values	8	4.8	2640	9.5	3.06

Table 2. Creep parameters of rocks mass.

Parameters	Activation energy, Q	Zone temperature, T	Gas constant, R	WIPP-Model constant, D
Units	J · mol^{-1}	K	J · mol^{-1} · K^{-1}	Pa^{-n} · s^{-1}
Values	50160	300	1.987	28.95e-36

Parameters	WIPP-model constant, A	WIPP-model constant, B	WIPP-model exponent, n
Values	22.8	25.4	4.9

Parameters	Material parameter, q_φ	Material parameter, q_k	Critical steady-state creep rate
Values	0.55	0.5	1.078 e-8

respectively. The cables near corner deviated 20° from normal direction of wall to corner. According to relative references (Liu, J.H et al. 2005, Liu, T.S et al. 2005), mechanical parameters and creep parameters of rocks mass were chosen and listed in table 1 and table 2; mechanical parameters of cables and anchors were listed in table 3. Following 4 reinforcement measurement methods were investigated by numerical simulation: method A was for naked roadway intersection, method B and C were for bolted roadway intersection without and with cables applied in floor at two corners, and the last method was method C companied with exerted pressure against floor, the pressure values ranged from 0.1 MPa to 1.0 MPa with interval of 0.1 MPa.

Table 3. Mechanical parameters of cables and anchors.

Parameters	Elastic modulus MPa	Grout cohesion strength MPa	Grout exposed perimeter m
Cable	45	0.2	1
Anchor	195	0.42	1

Parameters	Tensile strength MPa	Grout stiffness MPa	Cross-section area m$^2 \times 10^{-6}$
Cable	0.25	17.5	254
Anchor	1.85e3	5.35e3	249

3 RESULTS

3.1 *Analysis of creep stages*

XU et al. (2007) discussed that deformation process of the roadway can be divided into three stages including adjustment deformation stage, stable defor mation stage and accelerated deformation stage by investigation in the field.

Figure 6 shows deformations of naked roadway intersection versus creep time curves under different critical values. When $\varepsilon_{pt} > \varepsilon_{pc}$, Figure 6a illustrates that creep curves can be divided into two creep stages named initial creep stage and softening creep stage respectively, and each stage include a decelerated creep stage and a stable creep stage. At initial creep stage where the shear plastic value is lower than the critical value, deformation increases rapidly and then comes to a nearly constant value until shear plastic value exceeds the critical value. At softening creep stage, deformation of the roadway intersection increases rapidly with creep time for a longer period, and comes to stable state finally. Therefore, we can explain the case mentioned in section 1 that the deformation is little before a certain time, but increases at a high speed later.

For naked roadway intersection, when $\varepsilon_{pt} < \varepsilon_{pc}$, only initial creep stage occurs (see Fig. 6b). Roof deformation raises rapidly with a gradual decreasing velocity, then approaches a relatively constant value while the deformation velocity come to about 0; floor heave raises rapidly also, but it reaches a peak value, then decreases a little, finally come to a lower constant value. There is a deformation rebound in the deformation process of floor heave.

When $\varepsilon_{pt} > \varepsilon_{pc}$, and roadway intersection is reinforced by bolting and exerting pressure against floor, the relationships between deformation and creep time are shown in Figure 6c. Figure 6c illustrates that the

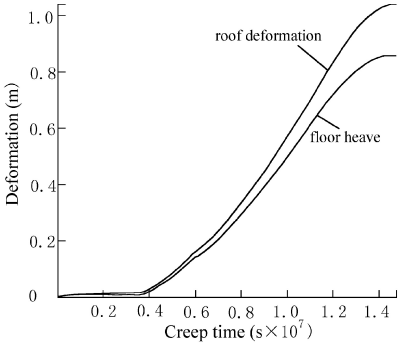

(a) $\varepsilon_{pt} > \varepsilon_{pc}$, for naked roadway intersection.

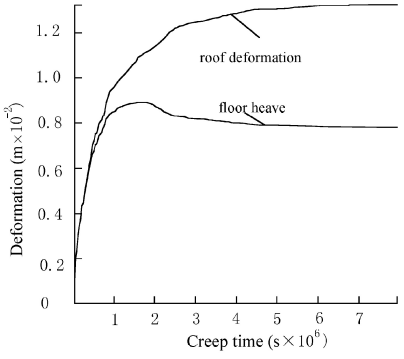

(b) $\varepsilon_{pt} < \varepsilon_{pc}$, for naked roadway intersection.

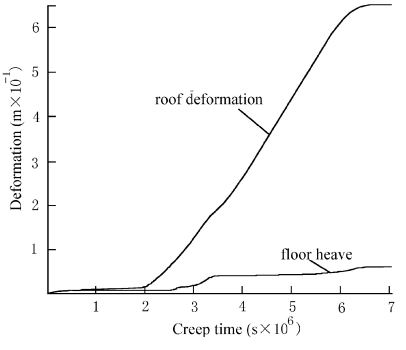

(c) $\varepsilon_{pt} > \varepsilon_{pc}$, for roadway intersection with reinforcement measurement.

Figure 6. Deformation-creep time curves under three conditions, ε_{pt} represents total shear plastic train value.

floor heave is very little compared with roof deformation; the profile of roof deformation is similar with that shown in Figure 6a, yet floor heave curve is very different. The beginning time of softening creep stage takes place late compared with that of roof deformation, and its total deformation value is less greatly than that of roadway intersection without reinforcement shown in Figure 6a. Therefore, Reinforcement for floor can reduce floor heave effectively.

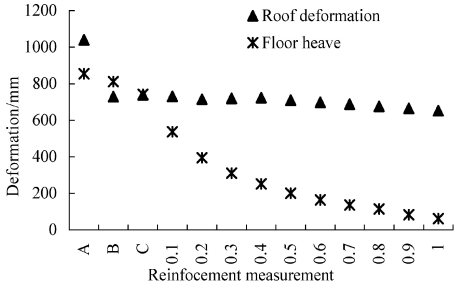

(a) Relationship between deformation and reinforcement methods.

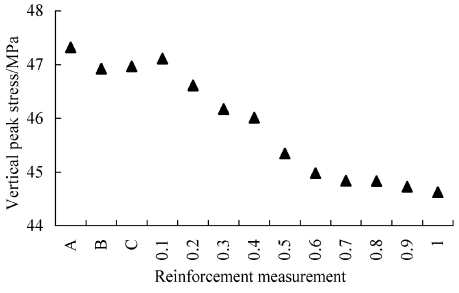

(b) Relationship between vertical peak stress and reinforcement methods.

Figure 7. The relationships between deformations, vertical stress peak value and reinforcement measurement: A, B and C represent Method A, method B and method C described in section 2.2; 0.1 ~ 1.0 MPa refer to the pressure values exerted against floor based on method C.

3.2 *Controlling technique*

Figure 7 illustrates that roof deformation decreases abruptly when naked roadway intersection are reinforced by bolting in roof and ribs, yet other reinforcement measurements have little affection on it; floor heave decreases a little when naked roadway intersection are reinforced by bolting in roof and ribs, even when cables were applied in floor near two corners (see Fig.7a), but floor heave lessens obviously with increment of pressure value exerted on the floor, and vertical stress peak value around roadway intersection also decreases (see Fig.7b); vertical stress peak values around roadway intersection with reinforcement measurement are all lower than naked roadway intersection. Only when the pressure value against floor is 0.1 Mpa and with reinforcement measurement method C, the vertical stress peak value has a little rebound. Therefore, we can reduce floor heave amount by exerting pressure against floor together with bolting support. If it is not enough yet, measurements of vertical cutting in floor (Guo, unpubl.) and so on can be used additionally.

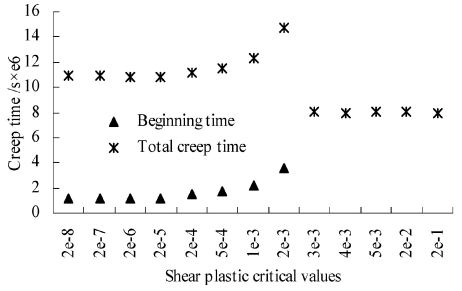

(a) Relationships between the beginning time of the second creep stage and total creep time and shear plastic critical value.

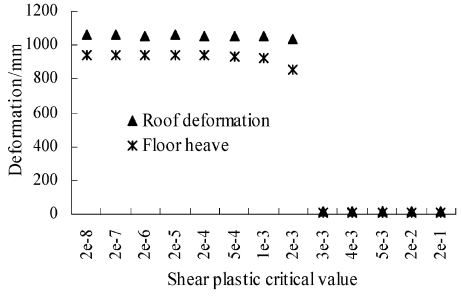

(b) Relationship between total deformation and shear plastic critical value.

Figure 8. Relationship between creep time, total deformation and shear plastic critical value.

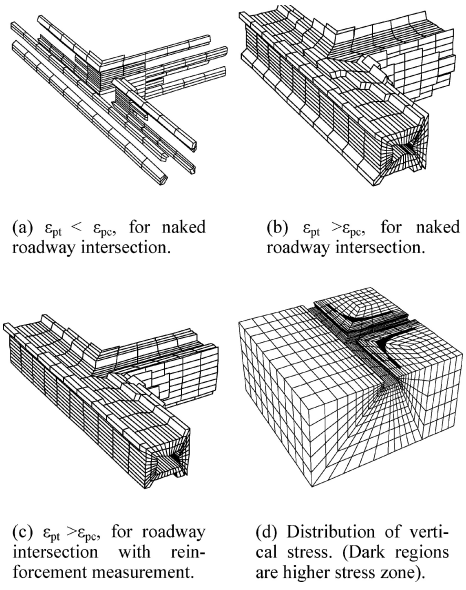

(a) $\varepsilon_{pt} < \varepsilon_{pc}$, for naked roadway intersection.

(b) $\varepsilon_{pt} > \varepsilon_{pc}$, for naked roadway intersection.

(c) $\varepsilon_{pt} > \varepsilon_{pc}$, for roadway intersection with reinforcement measurement.

(d) Distribution of vertical stress. (Dark regions are higher stress zone).

Figure 9. Distribution of higher vertical stress and softening zone distributions under three conditions.

4 DISCUSSION

4.1 *Affection of shear plastic critical value*

It is very important to choose reasonable shear plastic critical value when numerical simulation is performed. Figure 8 illustrates that when the critical value is above 2e-3, the second creep stage doesn't occur, and the deformation of the roadway intersection is very little, and the total creep time that calculation last is shorter. Otherwise, the second creep stage takes place. At the second creep stage, the deformation of the roadway intersection is larger and the deformation value of each critical value seems to be similar. But along with increment of the critical value, the beginning and end time of the softening creep stage delay a little, and total deformation lower a little. In summary, the shear plastic critical value determines if the softening creep stage takes place, and has a key influence on the beginning time, end time and total deformation of the second creep stage. So creep deformation of roadway intersection can be reduced by improving the shear plastic value.

4.2 *Generation mechanics of creep stages*

Research workers (Zhu et al. 2002, Wang et al. 2004, Li et al. 2006, Fan 2007) considered that rocks samples will failure finally if shear plastic value is large enough. Why can roadway intersection come to stable state finally?

Distribution of shear plastic zones (i.e. softening zone (Wang et al. 2004)) and vertical stress filed are plotted in Figure 9. As the results shown in Figure 9, the final shear plastic zone is small when $\varepsilon_{pt} < \varepsilon_{pc}$ (see Fig. 9a), greater when $\varepsilon_{pt} > \varepsilon_{pc}$ (see Fig. 9b), and can be reduced by reinforcement measurements (see Fig. 9c). When rocks mass in the softening zone lost their bearing capacity to some extent, adjacent rocks mass must provide more bearing capacity, if they can't, they will be softened also, and overburden pressure will continue seeking another rocks mass until the rocks mass can bear it sufficiently and keep stable finally (see Fig. 9d). Along with softening zone's generation and enlargement, peak stress value in surrounding rocks mass increases and its location diverts to rocks mass that hasn't been softened. All in all, although softened rocks mass adjacent to excavated room lost bearing capacity at a different degree, but rocks mass adjacent to softened rocks mass provide higher bearing capacity, so that the construction of roadway intersection do not lost its stability completely.

5 CONCLUSIONS

The conclusions of this research are summarized below:

1. Pwipp model of flac^{3D} software can be used effectively to simulate creep deformation of roadway intersection in deep mine. Strain-softening used

in this study includes softening of strength and deformation modulus.

2. Creep deformation-creep time curves can be divided into two stages including initial creep stage and softening creep stage, and only when total shear plastic value exceeds shear plastic critical value can softening creep stage occur. Determination of the critical value is very important in calculation, and creep deformation of roadway intersection can be reduced by means of improving the shear plastic value.
3. Bolting in surrounding rocks mass and exerting pressure against floor can reduce deformation of roadway intersection in deep mine. Method of exerting pressure against floor has more obvious effects to reduce floor heave than other measurements used in this research, if it is not enough, other measurement can be used additionally.

ACKNOWLEDGEMENTS

This work was carried out under the Outstanding Talent Innovation Fund of Henan province (No. 0621000400).

REFERENCES

Chen, Z.J. & Yang, J.W. 2005. Measures for supporting deep High Stress crack-expansion creep rock mass in Jinchuan mining district. Metal Mine (1): 18–22.

Cheng, R.H., Qian, M.G. & Miao, X.X. 2005. Numerical simulation in mining pressure control of thick and strong stratum caving by water-infusion softening method. Chinese Journal of Rock Mechanics and Engineering 24(13):2266–2271.

Fan, Q.Z. 2007. Experimental study on creep and its disturbed effect of rocks. Chinese Journal of Rock Mechanics and Engineering 26(1):216–216.

Li, Y.J., Pan, Y.S. & Zhang, M.T. 2006. Time effect on zonal disintegration process of deep rock mass. The Chinese Journal of Geological Hazard and control 17(4): 119–122.

Liang, Z.Z., Yang, T.H. & Tang, C.A. et al. 2005. Three-dimensional damage soften model for failure process of heterogeneous rocks and associated numerical simulation. Chinese Journal of Geotechnical Engineering 27(12): 1447–1452.

Liu, J.H., Zhu, W.S. & Li, S.C. et al. 2005. Analysis of rheological characteristics and stability of surrounding rock masses of Xiaolangdi hydrojunction underground caverns by using Flac3D. Chinese Journal of Rock Mechanics and Engineering 24(14): 2484–2489.

Liu, T.S., Zhao, J.Z. & Yang, J.E. et al. 2005. Support technology of bolt and anchor truss applied in large chamber of Tangkou mine. Coal Science and Technology 33(5):12–15.

Qiang, H., Zhou, H.Q. & Chang, Q.L. 2006. Regress analysis of mechanics characteristic of the rock strength at the pre-peak and post-peak. JiangXi Coal Science & Technology (2): 48–50.

Wang, H.P., Gao, Y.F. & Li, S.C. 2007. Uniaxial experiment study on mechanical properties of reinforced broken rocks pre-and-post grouting. Chinese Journal of Underground Space and Engineering 3(1): 27–31, 39.

Wang, J.A., Jiao, S.H. & Xie, G.X. 2006. Study on influence of mining rate on stress environment in surrounding rock of mechanized top caving mining face. Chinese Journal of Rock Mechanics and Engineering 25(6): 1118–1126.

Wang, J.J., Lu, Z.Y. & Liu, X.F. 2005. Discussion on floor upheaval mechanism of mine soft rock roadway. Coal Engineering (9): 67–68.

Wang, L.G., Wang Y.J. & Liu, X. 1994. The rheological instability theory for rock sample and its criteria. Journal of Fuxin Mining Institute (Natural Science) 13(3):93–97.

Wang, X.Q., Yang, L.D. & Gao, W.H. 2004. Creep damage mechanism and back analysis of optimum support time for soften rock mass. Chinese Journal of Rock Mechanics and Engineering 23(5): 793–796.

Xiao, H.F., He, X.Q. & Feng, T. et al. 2005. Research on coupling laws between EME and stress fields during deformation and fracture of mine tunnel excavation by Flac3D simulation. Chinese Journal of Rock Mechanics and Engineering 24(5):812–817.

Xu, X.L., Zhang, N. & Xu, J.G. et al. 2007. Principle and practice of process control over soft broken roadway with high ground stress. Journal of Mining & Safety Engineering 24 (1):51–55.

Yang, C., Chui, X.M. & Xu, S.P. 2002. Establishment and study of strain-softening numerical constitutive model for soft rock. Rock and Soil Mechanics 23 (6):695–697.

Yang, C.H. & Li, J.G. 2006. Analysis of creeping mechanisms of non-uniformity soft rocks. Journal of Mining and Safety Engineering 23(4):476–479.

You, M.Q. 2005. Study of deformation and failure of rock based on properties of cohesion and friction. Journal of Geomechanics 11(3):287–291.

You, M.Q. 2000. Strength of rock specimens and process of deformation and failure. Beijing: Geology Press.

Zeng, S., Yang, S.J. & Man, C. et al. 2005. Statistical constitutive model for limestone rock damage under uniaxial compression and its experimental study. Journal of Nanhua University (Science and Technology) 19(1): 69–72, 95.

Zhang, F., Dong, Z.H. & Ding, X.L. 2005. Numerical analysis of excavation process for tailrace tunnels of Pengshui project. Journal of Yangtze River Scientific Research Institute 22(6):59–62.

Zheng, Y.R. 2007. Discussion on yield and failure of geomaterials and stability analysis methods of slope/landslide – communion and discussion summary of special topic forum on geologic disasters in the three gorges project region. Chinese Journal of Rock Mechanics and Engineering 26(4):649–661.

Zhu, H.H. & Ye, B. 2002. Experimental study on mechanical properties of rock creep in saturation. Chinese Journal of Rock Mechanics and Engineering 21(12):1791–1796.

Zhu, Z. F. 1985. Stiff test machine. Beijing: coal industry press.